Acta Mechanica Slovaca **29 (2): 46 - 53,** June **2025**
https://doi.org/10.21496/ams.2025.013

Acta Mechanica Slovaca
ISSN 1335-2393
www.actamechanica.sk

Using a WEB-camera to Measure the Displacement of the Measuring Mark on a Rotating Object

Oleksandr Gorshenin

Zhytomyr Polytechnic State University, Chudnivska str., 103, Zhytomyr, Ukraine

Abstract: This paper provides a scientific justification for the potential to achieve a specified accuracy in measuring the spatial position of a tracking mark on a controlled rotating object using data from a cost-effective video camera. We conduct an error analysis of the displacement measurements of the tracking marker between consecutive frames in a video stream. A mathematical model is proposed to estimate the root mean square (RMS) error in the displacement of the marker within the image plane for a remote, non-contact position measurement sensor. This model accounts for camera parameters, marker characteristics, lighting conditions, and image distortions induced by motion and optical limitations of the lens. Our study demonstrates that high accuracy in measuring the angular position of an object is attainable through careful sensor design and optimal placement. Furthermore, we provide practical recommendations regarding the specifications of sensor components, tailored to the operational conditions and desired measurement accuracy.

Keywords: remote measurement; spatial position sensor; digital image processing; measurement errors; CMOS matrix light receiver; radiometric calculations; linear distortions in images; video stream frame.

1. Introduction

In modern automatic control systems for mechanical objects operating under challenging conditions, non-contact spatial position sensors video cameras equipped with matrix light receivers is used. The spatial position changes of the controlled object – such as displacement and rotation – are determined by tracking special markers across adjacent video frames through digital image processing and photogrammetry. These position changes are then converted into spatial data regarding the controlled object. Using of low-cost video camera-based sensors offers several advantages, including mechanical non-contact with the object, remote spatial position measurement, low cost, etc. However, the sensor's design must address specific accuracy requirements for measurements. Thus, there is a pressing need to provide a scientific foundation for achieving the desired accuracy in measuring the spatial position of markers on the controlled object using video camera data.

The mathematical foundation for measuring the displacement of an object's image in video frames relies on established digital image processing methods. Key algorithms are detailed in the works of Gonzalez and Woods [1], Forsyth and Ponce [2], and Jeahne [3]. Reference [4] discusses essential algorithms, methods, and practical techniques for filtering and radiometric transformations of digital images, as well as principles for correcting geometric distortions that arise during image acquisition. Additionally, [5] presents the design of a non-contact angular position sensor for a reference-

*** Corresponding author:** Oleksandr Gorshenin, ***E-mail address:*** *kktumtt_goe@ztu.edu.ua*

rotating device of a narrow-directional antenna in a space radio communication line, along with an experimental assessment of the sensor's accuracy.

Yurii Podchashynskyi has extensively addressed measurement accuracy from digital video images. Paper [6] explores improving measurement accuracy of rotational motion parameters of technical device elements (bodies of revolution) through algorithmic processing using linear approximation. Recommendations for image size and interframe interval are outlined in [7], confirming that non-contact motion parameter measurements can enhance process control. Lastly, paper [8] connects mathematical models of video images with measurement data of geometric parameters, proposing a method to determine model parameters and presenting experimental results within a control system.

Bilinsky Y. and Sukhotska I. in [9] propose an algorithm for determining and controlling geometric parameters of complex-shaped small objects by identifying subpixel coordinates in images. The total measurement error in the video surveillance system was 0.089 of a pixel size.

The development of a sensor for high-precision remote spatial measurement of an object necessitates specific design criteria and parameters for its components. These criteria are based on the sensor accuracy requirements set by the automatic control system. Measurement accuracy is evaluated through measurement errors, typically categorized in automatic control systems into dynamic and static errors. Dynamic error arises from changes in the object's state or position, while static error includes constant and random components. In deterministic control systems, the random component of the dynamic error is often neglected.

The purpose of the paper is to provide a scientific justification for the achievable accuracy of measuring changes in the spatial position of the measuring mark using adjacent frames of a video stream from a video camera that observes the mark on the object. The additional purpose is to provide recommendations for the selection of elements and design parameters of a remote sensor for the position of the measuring mark based on a cheap WEB camera.

2. Experimental Section

This section presents the theoretical justification for the mathematical error model, exemplified by a sensor designed for remote measurement of the angular position of a ground antenna system in a radio communication channel with a spacecraft in the X-band. The antenna must track a spacecraft moving at an angular velocity w_{ANT} up to 0.8 degrees per second. The accuracy requirements for antenna pointing are specified in angular minutes; for this example, the total permissible pointing error must not exceed 6 angular minutes [5]. Considering all components of the total error, the angular position sensor should have a measurement error of no more than 0.6 angular minutes.

The non-contact antenna rotation angle sensor uses an ordinary webcam to image capture the rotation scale of the ground antenna system for the low orbit spacecraft. The camera is mounted on a bracket opposite the antenna's azimuth or pitch scale. To achieve a clear image, the scale is illuminated by an LED spotlight. The scale consists of a brushed aluminium strip featuring black vertical degree marks, each 0.5 mm thick and spaced 4.3633 mm apart (Fig. 1). Scale ring diameter of 0.5 m. The main specifications of the light-sensitive CMOS matrix OV5640 (OmniVision), typical for webcams, are detailed in the manufacturer's documentation [10].

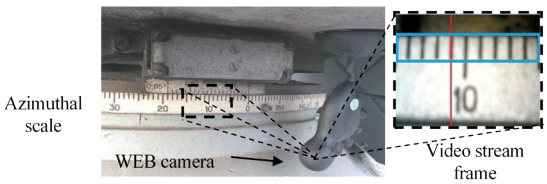

Figure 1: Image of the azimuthal scale of the rotation antenna system with the installed WEB camera.

An air layer, free of impurities and precipitation, exists between the camera and the scale surface. The camera is positioned so that the lines in the video frames align with the scale's movement direction, ensuring that the frame rows are perpendicular to the scale lines. The blue rectangle in Figure 1 delineates the evaluation window for a single frame, while the red line represents the current estimate of the scale line's position generated by the processing program.

Video streams are processed by a control computer, which selects neighbouring frames and averages pixel values within the analysis window by columns. The mutual correlation function of these

frames is then calculated to determine their relative shift based on the maximum correlation point. This shift is converted to both the relative angular shift and the absolute angular position of the antenna system. The calculated angular position is provided to the automated control system's algorithm as a measured value.

A experiment was conducted to evaluate the accuracy of a sensor designed for remote measurement of the rotation angle of a ground antenna system, utilizing a low-cost WEB video camera. The camera operated at a resolution of 320×240 pixels, and the experimentally determined root mean square measurement error was 3.96'. To estimate the image shift between frames, we employed a straightforward method to determine the position of a single halftone transition in the mark image.

3. Results and Discussion

The experimental results prompted further investigation into enhancing the accuracy of this angular rotation measurement method and adapting it for various control objects and additional spatial parameters. These objects may be situated in challenging environments or at significant distances. Such applications necessitate design calculations for camera selection based on specifications and optimization of its placement relative to the object while considering observation conditions. Thus, the study primarily focuses on establishing the relationship between sensor accuracy and the parameters of a WEB camera and its operating conditions.

The sensor's parameters are as follows: For the video camera, the key specifications include the number of CMOS elements in the light detector matrix (M rows and K columns), focal length f [m], lens aperture D [m], relative aperture $A = D/f$ or lens angle of view 2β. Additional characteristics are sensitivity V [mV/lux·c] or energy sensitivity V_e [μV/e], dynamic range DR [dB], maximum signal-to-noise ratio, digital-to-analogue converter (ADC) bit depth J, frame rate v [1/c], illumination E [lux], and integrated energy illumination E_0 [W/m^2] produced by the illuminator on the measuring mark's plane.

Several limitations are acknowledged in this study. We assume that the parameters and characteristics of the sensor remain constant or are controllable during operation. Therefore, constant components of statistical estimation errors are neglected, as they can be eliminated through calibration and algorithmic processing of video frame images and measurement results [4]. To assess the sensor's accuracy, we calculate the root mean square (RMS) error of the measurement marks' shift. The developed mathematical model accounts for various error components: statistical noise in the images, degradation of image quality due to sensor design, and dynamic error resulting from the movement of the mark during image accumulation. The general expression of the mathematical model considers the environmental effects on the propagation of light reflected from the marker.

To establish the key relationships between sensor parameters and the RMS of interframe displacement estimation errors, we first consider the model of the image signal generated by light reflected from the mark on the CMOS camera. Initially, we need to outline the basic assumptions. The illumination E (or integrated energy illumination E_0) of the mark (scale) across the entire camera field of view is uniform and sufficient for the operation of elementary photodetectors under typical light flux conditions. We disregard the spectral variations in illumination, reflection, absorption, and scattering within the camera's operating wavelength range. We assume that the camera output signal is a weighted sum of the RGB channels, with weighting factors adjusted to achieve uniform sensitivity across this range. Generally, we consider all coefficients and characteristics of the light receiver matrix, illumination, and light fluxes to be integral over the operating range. Assuming uniform reflectance across the entire background (brushed aluminium with the integral reflection coefficient $\rho_B \approx 0.5$) and the line field (black matte paint with the integral reflection coefficient $\rho_L \approx 0.1$), we consider these reflectance coefficients to be constant across all wavelengths ('perfect grey'). The length of the boundaries for the reflection coefficient transitions is negligible compared to the measurement error (perfect pattern of marks). To account for potential measurement ambiguity due to a periodic mark (scale), it is assumed that the mark cannot move more than one spatial period of the repeated pattern (distance between lines) during the time interval between frames. To enhance clarity, the mathematical models are initially presented in one-dimensional form, corresponding to a row of

light-sensitive elements in the camera sensor. To extend this to two dimensions, the formulas can be duplicated with a substitution of the coordinate variable.

Under these assumptions, the light distribution along a line of photosensitive elements in the camera's matrix photodetector can be represented as a series of illumination pulses resulting from reflection off a light background E_B and a dark line E_L. Figure 2 illustrates this: the top part shows a model image of mark lines for multiple row of the CMOS matrix; the bottom part displays a graph of illumination changes along the row (solid line) alongside an idealized graph (dashed line), which omits linear distortions from the lens and intermediate layer. The x-axis marks the positions of the photosensitive elements in the CMOS matrix. A table below indicates the signal value (in %) accumulated during the frame duration for the corresponding pixels, with cells related to the brightness transition zone (transition curve) shaded grey.

To create a radiometric model for the errors in measuring mark shift per frame interval, it is essential to consider the processes affecting the illumination of the video camera's photosensitive elements. The illumination values E_B and E_L in the image plane can be calculated using the following formulas:

$$E_B = \tau_S \cdot \frac{E \cdot \rho_B}{\pi} \cdot \tau_L \cdot \left(\frac{D}{f}\right)^2 + E_S, \qquad (1)$$

$$E_L = \tau_S \cdot \frac{E \cdot \rho_L}{\pi} \cdot \tau_L \cdot \left(\frac{D}{f}\right)^2 + E_S. \qquad (2)$$

Here, D is the lens entrance pupil diameter [m], f is the focal length [m], τ_L is the lens transmittance, τ_S is the transmission coefficient of the medium between the lens and the scale, ρ_B is the integral reflection coefficient of the background material, ρ_L is the integral reflection coefficient of the scale paint, E is the illumination of the scale in the camera field of view [lux], and E_S is the illumination in the image plane from light scattered in the medium between the lens and the scale [lux]. This model component may also include contributions from external background illumination of the lens. In the described application, the lens-mark distance is small, allowing us to neglect the influence of the atmospheric air layer. Additionally, there is no external illumination of the lens under these conditions. In this case, in formulas (1, 2) we can assume that $\tau_S = 1$ and $E_S = 0$.

The voltages calculations performed for the OV5640 CMOS sensor according to the manufacturer's specifications [10] give the following results. For the matrix operating at a frame rate of 30 fps, the minimum output voltage in complete darkness Umin is 0.27 mV, while the maximum output voltage under bright conditions U_{max} is approximately 0.53 mV, corresponding to a maximum illumination level E_{max} of about 27.6 lux. When illuminated at 27.6 lux, the digitized signal should reach its maximum of 1023 in a 10-bit representation. To avoid overload, designers typically adjust the gain so that Umax is slightly lower, for example, setting the maximum digital value F_{max} to 1000. These adjustments dictate the illumination requirements for the mark on the

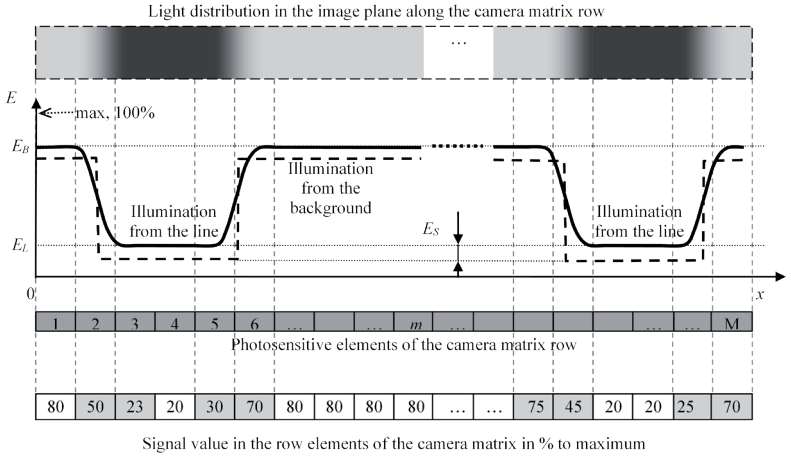

Figure 2: Perception of light signal by photosensitive elements of the light receiver matrix. The graph of illumination changes along the pixel line is shown as a solid line. The idealized illumination graph is a dotted line.

object, serving as specifications for the illuminator.

Figure 3 illustrates the model for optical signal formation at the light receiver matrix aperture $E(x,y)$, excluding linear distortions. The effects of linear distortions from a real lens, matrix, and mark movement will be discussed in subsequent sections.

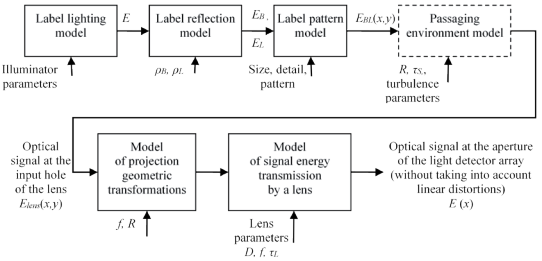

Figure 3: Schematic representation of the optical image formation model at the aperture of a matrix of photosensitive elements.

Assuming that the mark had a maximum light background, the maximum illumination value E_{BLmax} in the mark's plane can be calculated as follows:

$$E_{BL\max} = \frac{E_{\max} \cdot \pi}{\rho_B \cdot \tau_L} \cdot \left(\frac{f}{D}\right)^2 = \frac{E_{\max} \cdot \pi}{\rho_B \cdot \tau_L \cdot A^2} = \frac{U_{\max} \cdot \pi}{\rho_B \cdot \tau_L \cdot A^2 \cdot V \cdot t_K}, \quad (3)$$

where $A = D/f$ represents the lens's relative aperture.

Typical low-cost WEB cameras, such as the Waveshare OV5640 5MP USB, feature a lens with a relative aperture of f/2.8, a focal length of 3.29 mm, and a transmittance of approximately 0.85. For optimal performance with the OV5640 CMOS sensor, the tag illumination should be around 147 lux. This level can be achieved using a 0.3-0.5 W LED light with a 120° scattering angle, positioned 0.5 m from the scale.

The digital signal value from the dark paint F_L will be less than $\rho_B/\rho_L = 0.5/0.1 = 5$ times, yielding. $F_L \approx 200$. The calculated standard deviation of the noise in the digital stream signal is approximately 16.

To develop a spatial model of errors in measuring mark displacement per frame interval, it is essential to examine the formation of the mark image in the image plane, considering the spatial sampling of the signal. The light distribution signal $E(x)$ along the row of light-receiving elements is discretized with a step $\Delta x_D = X/M$, where X is the physical length of the photocell matrix row and M is the number of matrix elements. For the OV5640 matrix (1/4" diagonal), M is 1080 at a frame rate of 30 frames per second, with X measuring 3.2 mm, resulting in $\Delta x_D \approx 3$ µm. The sampling step in the image plane Δx_D corresponds to the sampling step in the object plane ΔX_D with a scale factor R/f, where R is the distance from the lens's main point to the subject plane and f is the lens's focal length.

The sharp dark-to-light transitions described theoretically permit precise mark position measurements. However, the actual image in the lens plane appears blurred due to several factors: defocusing from the space between the camera and the mark, mark movement during image signal accumulation, diffraction limitations of the lens, and lens aberrations. In the example considered, the effect of the turbulent layer between the camera and the mark is negligible. However, the diffraction limitations become significant, particularly for typical web cameras with an aperture diameter D of about 1 mm. For green light and a focal length of 3.89 mm, the theoretical diffraction spot width $2\sigma_L$ is approximately 2.61 µm:

$$2\sigma_L = 1{,}22 \cdot \frac{\lambda \cdot f}{D} = 1{,}22 \cdot \frac{0{,}550 \cdot 10^{-6} \cdot 3{,}89 \cdot 10^{-3}}{10^{-3}} \approx 2{,}61\ \mu\text{m}. \quad (4)$$

The estimate of the point spread function (PSF) width based solely on diffraction limitations is minimal; the actual PSF is typically two to three times wider due to lens aberrations. For our analysis, we will assume an axisymmetric PSF with a realistic width, particularly notable away from the main beam's intersection with the image plane, near the frame edges. Manufacturers often attempt to align the pitch of photosensitive elements in the sensor with the actual PSF width, although this is frequently challenging, especially in low-cost webcams. We will discuss this matching approach and the impact of photosensitive element spatial pitch in the following sections.

According to the sampling theorem, in the ideal case, recovering a sampled signal without loss requires that the sampling step allows the minimal image element to contain at least two samples. The smallest point in the image of a light signal is represented by a Gaussian PSF with parameters (x_0, y_0) for spatial position and (σ_x, σ_y) for spot width at approximately 0.606 of the maximum illumination value at point $E(x_0, y_0)$. To model this smearing, classified as a linear distortion in the image, a spatial low-pass linear filter with a Gaussian impulse

response $h_L(x)$ is typically employed:

$$h_L(x) = \exp\left(-\frac{x^2}{2\sigma_x^2}\right). \quad (5)$$

In this application, point objects are absent; instead, sharp transitions occur between "dark" and "light" backgrounds. Here, the PSF appears in a transition curve, which can be related to the PSF via an integral and represented by the probability integral function $\mathrm{erf}(x)$. The light distribution across the matrix along the x-coordinate $\mathrm{ET}(x)$, corresponding to the "dark-light" transition on the mark will be described as follows:

$$E_T(x) = (E_B - E_L)\frac{1}{2}\left[1 + erf\left(\frac{x}{\sqrt{2}\cdot\sigma_x}\right)\right] + E_S. \quad (6)$$

We establish the requirement for element spacing in the matrix based on the width of the transition curve, defined as $2\sigma_x$, measured at levels from approximately 0.16 to 0.84 of the range ($E_B - E_L$) of the transition curve. A matrix with an element spacing of Δx_D can discretize a light signal in the image plane without loss, provided the transition curve is at least $2\cdot\Delta x_D$ in length. In practical applications, video camera designers often select a sampling step that is 30-50% smaller than the based on sampling theory minimum. This can be verified by examining a halftone transition in a digital image characterized by a sharp reflectance jump. Observations should be made at high magnification in the centre of the frame using nearest neighbour interpolation. Usually, such the halftone transition typically spans at least three pixels.

The real aperture size $\Delta l \approx \Delta x_D$ causes smearing of halftone transitions in the sampled signal, which is equivalent to the action of a low-pass filter with a rectangular pulse response $h_D(x)$ of length $\Delta l \approx \Delta x_D$. This equivalent filter produces a linear transition instead of a sharp dark-to-light change.

The dynamic component causing blurring in dark-to-light transitions arises from the mark's movement during signal accumulation in the frame. This effect can be integrated into the image signal's mathematical model if the mark's spatial motion is known. Linear motion of the mark's image in the light detector's aperture plane results in linear smearing of the accumulated signal. Due to the linearity of the sampling operation, this smearing can be modeled as the action of a linear filter with a rectangular impulse response $h_m(x)$ on the continuous optical signal $E(x)$. The rectangle length lm in $h_m(x)$ corresponds to the distance the image moves during accumulation time, expressed by the

$$l_m = V_X \cdot t_K \cdot \left(f/R\right), \quad (7)$$

where V_X is the average speed of the mark in the subject plane [m/s], $t_K = 1/v_{\mathrm{frame}}$ is the signal accumulation time, and f/R represents the image scale.

In the case of the sensor under consideration, the calculation of l_m as follows: The maximum angular rotation speed of the antenna w_{ANT} according to the requirements is 0.8 deg/s. Such a rotation for the frame duration $t_K = 1/30 \approx 0.033$ c will cause a linear displacement of the scale surface by approximately 0.12 mm. If the above-mentioned camera is placed at a distance R=100 mm from the scale, this mark displacement corresponds to an image blur of about $4\cdot10^{-3}$ mm. This shift of the optical image per frame corresponds to a shift of 4/1.4 ≈ 3 pixels on the digital image.

The total equivalent linear distortion (smearing) in an optical image is a result of three factors: diffraction limits and lens aberrations, real sampling limitations, and image motion during signal accumulation. These linear distortions are modeled as the convolution of an "ideal" light signal $E(x)$ with the impulse responses of linear filters that represent each factor. A diagram illustrating the linear distortion model in a digital image, as well as the sampling and analogue-to-digital conversion processes, is presented in Figure 4.

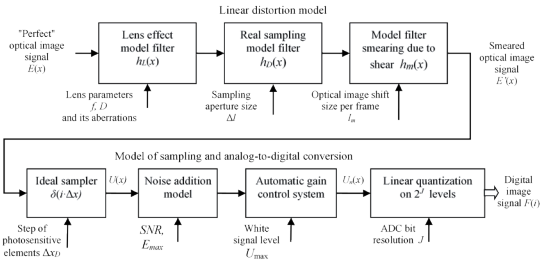

Figure 4: Schematic of the model of linear distortions in a digital with a model of sampling and analog-to-digital conversion.

Considering lens aberrations and the maximum blur from movement, the transition length can reach $\Delta l_{max} \approx 13.2$ μm, corresponding to a blur of 9 pixels in discrete representation. For a camera positioned 0.1 m from the scale, this translates to approximately

0.34 mm on the mark's surface, which is slightly more than half the width of the scale line. In terms of the antenna's rotation angle, this equates to 4.7 arc minutes.

The position of the measuring mark in the current frame is determined using software algorithms. For greater accuracy in measuring the spatial displacement of the mark (Δx) relative to its position in the previous frame, we recommend assessing the maximum of the mutual correlation function (MCF) of the images along the x-axis in the previous $E_{i-1}(x)$ and current $E_i(x)$ frames. Calculating the MCF of light signals in adjacent frames effectively compresses the light signal using an optimal filter. This involves a digital convolution algorithm, typically implemented via fast discrete Fourier transform techniques.

Theoretical principles of signal processing indicate that with a good signal-to-noise ratio, the error distribution for measuring the maximum position x_{max} of a signal compressed by the optimal filter follows a normal (Gaussian) distribution. The Rao-Kramer lower bound for the standard error (SE) of the measurement this measurement for a single signal pulse (for one light spot from the point or for one dark-to-light transition) is given by

$$SE_x \geq \frac{1}{2\pi\sqrt{2}q \cdot W_e}, \qquad (8)$$

where q is the signal-to-noise ratio (SNR), W_e is the effective width of the signal spatial spectrum.

The effective width of the spatial spectrum W_e of the light signal sampled by the matrix can be estimated as the inverse of the width of the transition curve Δl. Then

$$SE_x \geq \frac{\Delta l}{2\pi\sqrt{2}q}. \qquad (9)$$

In the current example, the digital signal $F(i)$ from a 10-bit video stream of a WEB camera with an OV5640 sensor has a signal-to-noise ratio of $q \approx (1000-200)/16 = 50$. For an optimistic estimate, we calculate the PSF width, neglecting lens aberrations and motion blur, as $\Delta l = \sigma_x + \Delta x_D \approx 4$ μm. Consequently, the optimistic estimate for the standard error of the image displacement measurement in the image plane is $4/(50 \cdot 8.889) \approx 0.009$ μm. Considering maximum movement and real lens aberrations – up to three times larger than the diffraction spot – the pessimistic estimate of the measurement error may reach ≈ 0.03 μm.

Calculating the MCF for a group of N halftone transitions in a frame line (see Fig. 1) increases the signal-to-noise ratio by a factor of $N^{1/2}$ due to incoherent accumulation. In this case, $N = 2 \cdot (N_{mark}-1)$, where N_{mark} is the number of mark dashes within the analysis window. A reduction of N_{mark} by 1 was made to account for boundary effects. N_{mark} also depends on the width of the frame projection on the mark and the distance between the mark dashes. In the current example, for a camera positioned 0.1 m from the scale, the theoretical number of accumulated signals (halftone transitions) is 36. The pessimistic estimate of the standard error in measuring the mark's position in the image plane could be as high as 5 nm.

When selecting a camera installation location (distance R), several factors must be considered. The signal-to-noise ratio improves with the number of marked elements according to a square root function, and significant increases in signal quality only occur with fewer than 10 marker dashes. If the marker is not planar, increasing the frame size leads to rapid geometric and linear distortions at the edges. Additionally, webcams typically have a minimum focusing distance of 0.1-0.2 m, and focusing at short distances exacerbates these distortions. Therefore, the processed spatial signal should be confined to a window in the centre of the frame.

If the recommendations for a window width of 10 dashes are implemented, the pessimistic estimate of the standard error in the image shift measurement, considering lens aberrations and image motion, is approximately 10 nm. For R = 0.1 m on the surface of the mark scale this means an SE of approximately 0.26 μm, which corresponds to an error in the measurement of the antenna rotation of 0.216 arc seconds. This theoretical estimate is exceptionally small. However, in practical design, factors such as discrepancies in the mark pattern, potential sensor vibrations, and flaws in the rotation mechanism must be considered.

4. Conclusions

The evaluation of the theoretically achievable accuracy for measuring the angular position of a control object using a sensor based on a web camera indicates promising prospects for its application in control systems for mechanical objects. This assessment employed a mathematical

model specifically developed for this purpose, accounting for both the radiometric characteristics of the camera and linear distortions (such as image smearing) that occur in practical scenarios. In the case of an inexpensive web camera equipped with an OV5640 photosensitive matrix, utilizing correlation methods for image frame processing, the pessimistic estimate of the standard error in measuring the position of the mark on the matrix plane is 5 nm.

The model was validated using a practical non-contact rotation angle sensor based on a web camera, which monitors the measuring scale of a ground-based antenna system within a radio communication channel with a spacecraft. The results affirm the adequacy of the model. The developed model, along with practical recommendations for selecting sensor components and parameters presented in this paper, can serve as a foundation for the development of new sensors for remote measurement of the marks spatial position.

References

1. Gonzalez, R. C., Woods, R. E. (2018). Digital Image Processing, 4rth edition. Pearson Education Limited, London.
2. Forsyth, D., Ponce, J. (2011). Computer Vision: A Modern Approach, 2nd Edition. Pearson Education, London.
3. Jeahne, B. (2004). Practical Handbook on Image Processing for Scientic and Technical Applications, 2nd edition. CRC Press LLC, Boca Raton, Florida, United States.
4. Gorshenin, O., Dubyna, O., Kondratenko, S., Boloban, S. (2007). Tsyfrova obrobka zobrazhen ta osnovy fotohrammetrii. ZhVIRE, Zhytomyr, Ukraine.
5. Gorshenin, O. Ye., (2024). Bezkontaktnyi datchyk kutovoho polozhennia oporno-povertalnoho prystroiu vuzkospriamovanoi anteny. XIV Mizhnarodna naukovo-technichna konfarencija "Informatsiino-kompiuterni tekhnolohii – 2024", 28–29 March, Zhytomyr, Ukraina. Zhytomyr: «Zhytomyrska politekhnika», 178–179.
6. Podchashynskyi, Yu. O. (2009). Pidvyshchennia tochnosti vymiriuvan parametriv obertovoho rukhu na osnovi alhorytmichnoi obrobky dvovymirnoi vymiriuvalnoi informatsii. Eastern-European Journal of Enterprise Technologies, 1(3(37)), 17–22.
7. Podchashynskyi, Y., Luhovykh, O., Tsyporenko, V. and Tsyporenko, V. (2021). Devising a method for measuring the motion parameters of industrial equipment in the quarry using adaptive parameters of a video sequence. Eastern-European Journal of Enterprise Technologies, 6(9(114)), 32–46.
8. Korobiichuk, I., Podchashinskiy, Y. (2021). Correlation mathematical model of video images with measuring information about geometrical parameters. 25th International Conference on Methods and Models in Automation and Robotics, MMAR, 23–26 Aug, 59–63.
9. Bilynskyi, Y. Y., Sukhotska, I. V. (2015). Alhorytm vyznachennia ta kontroliu heometrychnykh parametriv malohabarytnykh obiektiv skladnoi formy shliakhom subpikselnoi obrobky yikh zobrazhen. Metody ta prylady kontroliu yakosti, 1(34), 71–77.
10. OmniVision Technologies, Inc. Color CMOS QSXGA (5 megapixel) image sensor with OmniBSI™ technology. Datasheet (CSP3). Preliminary specification. Version 1.0. February 2010, from https://www.uctronics.com/download/Image_Sensor/OV5640_CSP3_DS.pdf.